Primary cilia in stem cells and neural progenitors are regulated by neutral sphingomyelinase 2 and ceramide

Qian He[a], Guanghu Wang[a], Sushama Wakade[a], Somsankar Dasgupta[a], Michael Dinkins[a], Ji Na Kong[a], Stefka D. Spassieva[b], and Erhard Bieberich[a]

[a]Program in Developmental Neurobiology, Department of Neuroscience and Regenerative Medicine, Medical College of Georgia, Georgia Regents University, Augusta, GA 30912; [b]Division of Hematology/Oncology, Department of Medicine, Medical University of South Carolina, Charleston, SC 29425

ABSTRACT **We show here that human embryonic stem (ES) and induced pluripotent stem cell–derived neuroprogenitors (NPs) develop primary cilia. Ciliogenesis depends on the sphingolipid ceramide and its interaction with atypical PKC (aPKC), both of which distribute to the primary cilium and the apicolateral cell membrane in NP rosettes. Neural differentiation of human ES cells to NPs is concurrent with a threefold elevation of ceramide—in particular, saturated, long-chain $C_{16:0}$ ceramide (*N*-palmitoyl sphingosine) and nonsaturated, very long chain $C_{24:1}$ ceramide (*N*-nervonoyl sphingosine). Decreasing ceramide levels by inhibiting ceramide synthase or neutral sphingomyelinase 2 leads to translocation of membrane-bound aPKC to the cytosol, concurrent with its activation and the phosphorylation of its substrate Aurora kinase A (AurA). Inhibition of aPKC, AurA, or a downstream target of AurA, HDAC6, restores ciliogenesis in ceramide-depleted cells. Of importance, addition of exogenous $C_{24:1}$ ceramide reestablishes membrane association of aPKC, restores primary cilia, and accelerates neural process formation. Taken together, these results suggest that ceramide prevents activation of HDAC6 by cytosolic aPKC and AurA, which promotes acetylation of tubulin in primary cilia and, potentially, neural processes. This is the first report on the critical role of ceramide generated by nSMase2 in stem cell ciliogenesis and differentiation.**

Monitoring Editor
Howard Riezman
University of Geneva

Received: Dec 20, 2013
Revised: Feb 25, 2014
Accepted: Mar 27, 2014

INTRODUCTION

Human embryonic stem (ES) cells have great potential for the treatment of a wide range of rare and common diseases, such as cancer, cardiac muscle infarction, and diseases of the nervous system. They are also bona fide in vitro model systems for studying differentiation processes in embryo development. Despite this progress in understanding stem cell differentiation, it is not clearly understood how stem cells differentiate into various spatially organized tissues and organs. Recently primary cilia have been shown to regulate cell signaling pathways critical for embryo morphology and development (Rohatgi *et al.*, 2007; Han and Alvarez-Buylla, 2010; Komatsu and Mishina, 2013).

The nonmotile primary cilium appears as a single-membrane protrusion in eukaryotic cells. The axoneme of the primary cilium consists of a 9+0 microtubule structure, different from the 9+2 arrangement of the motile cilium (Pan and Snell, 2007; Gerdes *et al.*, 2009; Satir *et al.*, 2010). Primary cilia have a defined location on epithelial cells (mostly apical). Of importance, they are studded with various growth factor receptors, such as receptors for platelet-derived growth factor and sonic hedgehog cell signaling pathways. Because these signaling pathways are important for neural differentiation and brain development, primary cilia on neural stem and progenitor cells are critical for regulating the spatially organized differentiation and morphology of neural tissues.

There is growing evidence that the sphingolipid ceramide regulates ciliogenesis by being compartmentalized to a ceramide-enriched

This article was published online ahead of print in MBoC in Press (http://www.molbiolcell.org/cgi/doi/10.1091/mbc.E13-12-0730) on April 2, 2014.

Address correspondence to: Erhard Bieberich (ebieberich@gru.edu); Stefka D. Spassieva (spassisd@musc.edu).

Abbreviations used: ACEC, apical ceramide-enriched compartment; aPKC, atypical protein kinase C; AurA, Aurora A kinase; ES, embryonic stem; FB1, fumonisin B1; HDAC, histone deacetylase; iPS, induced pluripotent stem; MDCK, Madin–Darby canine kidney; NP, neural progenitor; nSMase, neutral sphingomyelinase; TSA, trichostatin.

apical compartment (ACEC) as described for polarized Madin–Darby canine kidney (MDCK) cells (Wang *et al.*, 2009a; He *et al.*, 2012). In these cells, ceramide is derived from endolysosomal degradation of sphingomyelin by acid sphingomyelinase and promotes ciliogenesis by inducing the formation of a ciliogenic ceramide–protein complex. However, it is not known whether this mechanism is also active in other cell types—in particular, in differentiating human ES cells.

Based on immunocytochemistry using antibodies with high affinity to very long chain $C_{24:0}$ and $C_{24:1}$ ceramide (*N*-lignoceryl and nervonoyl D-erythro sphingosine; see Supplemental Figure S1 for structures) and subcellular fractionation studies, our results suggest that very long chain ceramide sequesters atypical PKC (aPKC) to the cell membrane, thereby preventing activation of HDAC6 by a cytosolic isoform of aPKC. Therefore we describe a previously undescribed, unexpected, and novel function of $C_{24:1}$ ceramide and its interaction with aPKC in ciliogenesis of human ES cell–derived neural progenitor (NP) cells. Most surprisingly, $C_{24:1}$ ceramide promotes primary cilium and neural process formation, indicating a critical role of very long chain ceramide in neural stem and progenitor cell differentiation.

RESULTS

Ceramide colocalizes with acetylated tubulin in primary cilia and the mitotic spindle of human ES cells

Primary cilia are reported in undifferentiated human ES cells (Kiprilov *et al.*, 2008). However, their formation and regulation in human ES cell–derived NPs is not known. We previously found that ceramide is important for ciliogenesis in MDCK cells, suggesting that ceramide is also critical for regulation of primary cilia in differentiating human ES cells (Wang *et al.*, 2009a; He *et al.*, 2012). We tested the formation of primary cilia and their association with ceramide in undifferentiated ES cells and ES cell–derived NPs. The ES cells were first cultivated on mouse embryonic fibroblasts (MEFs) and then transferred to feeder-free conditions using Geltrex as the matrix. When undifferentiated ES cells reached confluence, knockout serum replacement (KSR) was withdrawn for 10 h. Cells were fixed and then immunolabeled using antibodies against ceramide and the primary cilium marker acetylated tubulin. Figure 1A and Supplemental Figure S2 show that KSR deprivation induced the formation of short primary cilia in undifferentiated human ES cells, which were colocalized with ceramide. Of interest, ceramide was also colocalized with acetylated tubulin at the mitotic spindle (Figure 1B).

Next we tested the distribution of ceramide and its colocalization with acetylated tubulin in NPs differentiated from human ES cells. We followed different protocols for NP differentiation, including embryoid body–derived NPs and adherent monolayer cultures with SMAD inhibition and reduction of KSR to 5% without basic fibroblast growth factor (bFGF) supplementation (Dhara *et al.*, 2008; Dhara and Stice, 2008; Chambers *et al.*, 2009; Swistowski *et al.*, 2010). Figure 1, D and E, and Supplemental Figure S3 show that the differentiating ES cells expressed the intermediate filament protein nestin and the transcription factors Sox1 and Pax6, which are typical characteristics of NPs (Supplemental Figure S4). Consistent with undergoing neural differentiation, NPs did not express the pluripotency markers Oct-4 and Nanog (Supplemental Figure S4) but showed elevation of ceramide, which was distributed to the apical cell membrane and primary cilia (Figure 1, D and E, and Supplemental Figure S3). NPs adopted rosette morphology, which is another typical characteristic of neural differentiation (Figure 1, E and F). A *z*-scan of the NP rosettes clearly demonstrated that ceramide was distributed to apical vesicles and colocalized with acetylated tubulin (Figure 1F). These results suggested that ceramide generation was elevated during neural differentiation and that its distribution was to the apical membrane (Figure 1, E and F, and Supplemental Figure S4, A and B). Nestin was predominantly localized at the basal part of the rosette cells, thereby recapitulating the polarized distribution of ceramide and nestin in NPs of the ventricular zone (Wang *et al.*, 2008). Sphingolipidomics (liquid chromatography–tandem mass spectrometry [LC-MS/MS]) analyses showed that neural differentiation of human ES cells was concurrent with threefold elevation of total ceramide and the species $C_{16:0}$ and $C_{24:1}$ ceramide (Figure 2A). Therefore our data suggested that elevation of distinct ceramide species, in particular $C_{16:0}$ and $C_{24:1}$ ceramide, is important for neural differentiation of human ES cells.

Inhibition of ceramide generation leads to loss of primary cilia, which are restored by treatment with exogenous ceramide

To test the functional significance of ceramide for ciliogenesis, we used two inhibitors of ceramide-generating enzymes: fumonisin B1 (FB1) and GW4869, which inhibit ceramide synthase and neutral sphingomyelinase(s) (nSMase), respectively (Desai *et al.*, 2002; Marchesini *et al.*, 2003; Marasas *et al.*, 2004; Pruett *et al.*, 2008; Dobierzewska *et al.*, 2012). High-performance TLC (HPTLC) analysis of lipid extracts from ES cell–derived NPs verified that these inhibitors reduced total ceramide in NPs (Figure 2B and Supplemental Figure S5). Consistent with ceramide depletion, the number of primary cilia was diminished by FB1 and GW4869, as shown in Figure 2C. Exogenously added $C_{16:0}$ ceramide or its ceramide analogue (*N*-palmitoyl serinol, or S16) partially rescued ciliogenesis in inhibitor-treated cells. When added as a single ceramide species, $C_{24:1}$ ceramide was most effective in restoration of primary cilia, consistent with the observation that its concentration was fourfold to fivefold elevated during neural differentiation (Figure 2, A and C). Sphingolipidomics analysis showed that FB1 and $C_{24:1}$ ceramide–treated cells were enriched with $C_{24:1}$ ceramide as the major ceramide species, which was not converted to glycosphingolipids (Supplemental Figure S6). When combining exogenously added ceramide species, the most impressive effect was found with the combination of $C_{16:0}$ and $C_{24:1}$ ceramide (Figure 2C). Therefore our data indicated that particular ceramide species or their combination, namely $C_{16:0}$ and $C_{24:1}$ ceramide, but not ceramide derivatives such as glycosphingolipids, are important for ciliogenesis in differentiating human ES cells.

Ceramide depletion leads to loss of aPKC colocalization with ceramide at the primary cilium and the apicolateral cell membrane

On the basis of our previous observation that ceramide binds directly to aPKC, we tested whether aPKC colocalized with ceramide in ES cell–derived NPs (Bieberich *et al.*, 2000; Wang *et al.*, 2005, 2009b; He *et al.*, 2012). Figure 3 shows that aPKC colocalized with ceramide in the mitotic spindle of dividing cells (Figure 3, A and B) and with the primary cilium in ciliated cells (arrow in Figure 3C). In ciliated cells, there was also labeling of aPKC in the apicolateral membrane, which was not labeled for ceramide when using the anti-ceramide immunoglobulin M (IgM) antibody (arrowheads in Figure 3, C and D). We then treated differentiating human ES cells with FB1 or GW4869 to test whether ceramide depletion altered the membrane distribution of aPKC. Figure 3, E and F, shows that ceramide depletion led to translocation of aPKC to the cytosol, concurrent with loss of primary cilia, as indicated by diffuse (cytosolic) labeling for acetylated tubulin in FB1- and GW4869-treated cells. These results suggested that a distinct pool of ceramide in the apicolateral membrane was also affected by FB1 and GW4869, although this pool was not detectable with the anti-ceramide IgM

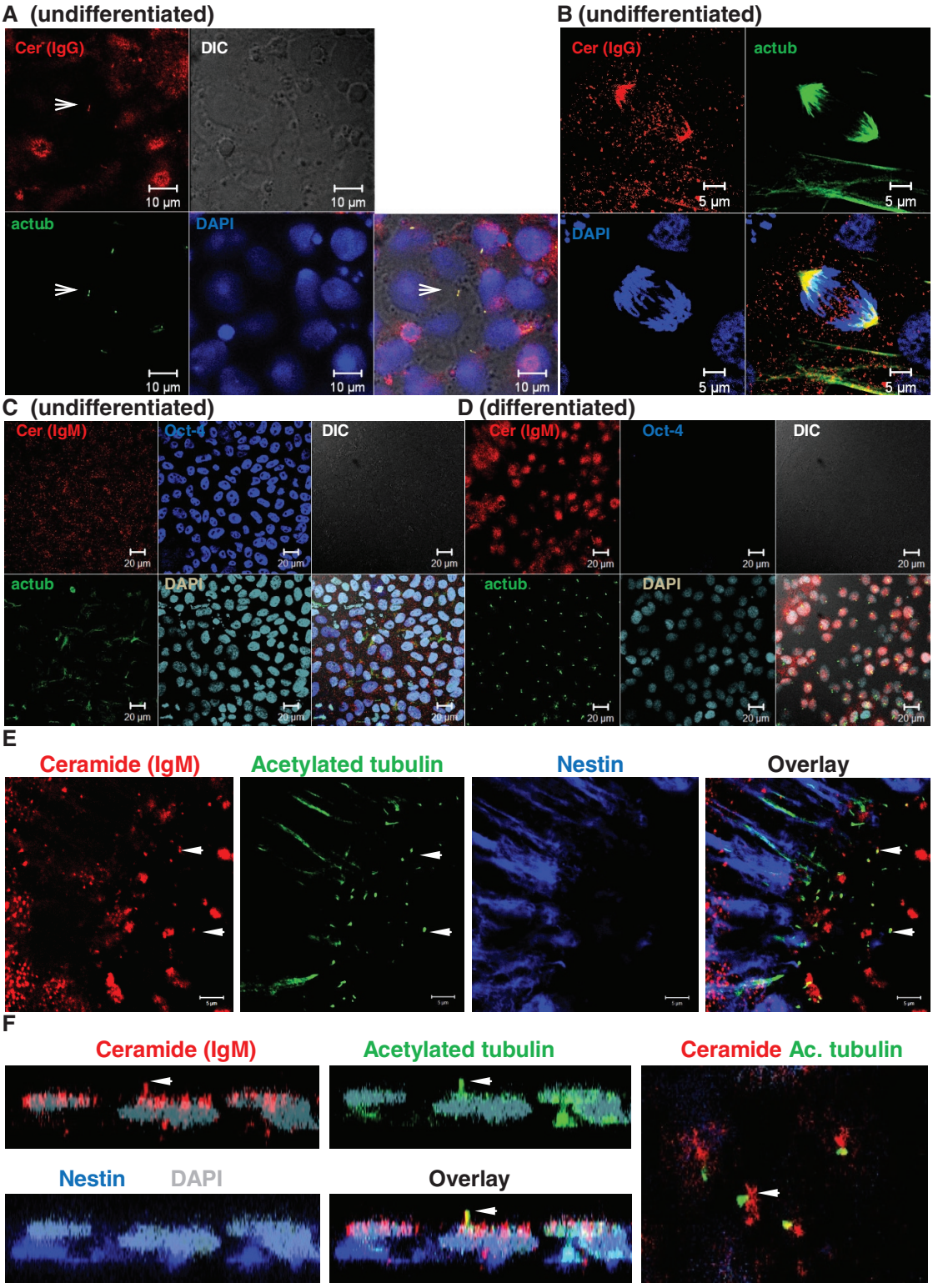

FIGURE 1: Ceramide is colocalized with acetylated tubulin in primary cilia and the mitotic spindle. Human ES cells were cultivated feeder free and then subjected to immunocytochemistry using antibodies against ceramide (rabbit IgG or mouse IgM, red) and acetylated tubulin (green). (A) Interphase; arrow points at primary cilium. Bar, 10 µm. (B) Metaphase. Bar, 5 µm. (C, D) Neural differentiation suppresses expression of Oct-4 concurrent with elevated expression of ceramide and formation of primary cilia (C is before and D is after neural differentiation). Bar, 20 µm. (E) Primary cilia are formed in nestin-expressing NPs in neural rosettes. In NPs, ceramide is colocalized with primary cilia and vesicles at the cilium bases (arrows). Bar, 5 µm. (F) A *z*-scan of individual cell in neural rosette. Arrow indicates colocalization of ceramide with acetylated tubulin in primary cilium. Right, apical plane of area used for *z*-scan.

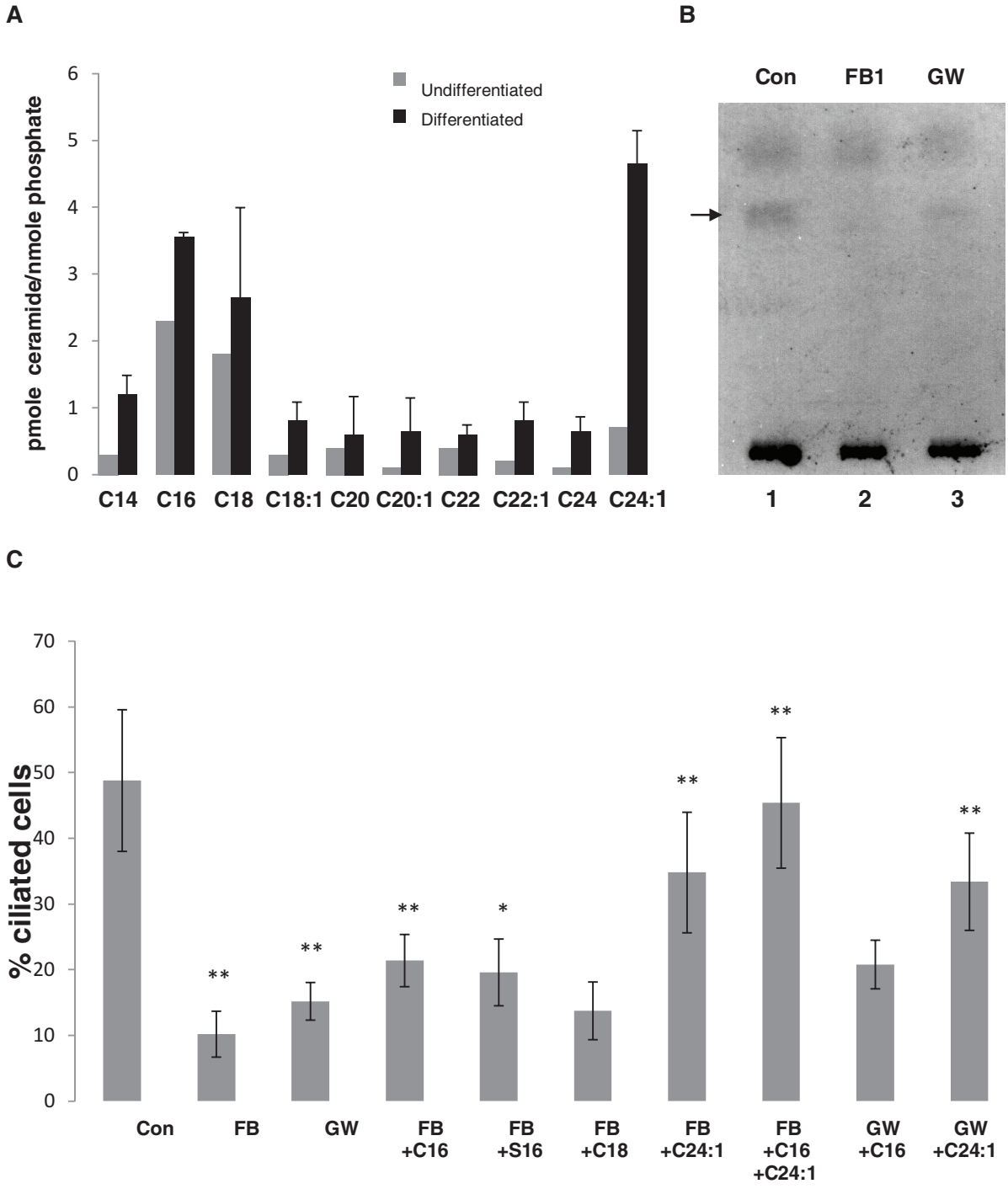

FIGURE 2: Ceramide depletion reduces ciliogenesis, whereas addition of ceramide rescues cilium formation. Mass spectrometric analysis of ceramide species in undifferentiated human ES cells and ES cell-derived NPs (A) and HPTLC analysis (B) of ceramide in NPs in the presence or absence of inhibitors for ceramide generation (FB1 or GW4869). Arrow in B points at ceramide band stained with cupric acetate/charring. (C) Proportion of ciliated cells (length of cilia >1 μm) in NPs with reduced ceramide levels and after the addition of exogenous ceramide (C16, $C_{16:0}$ ceramide; C18, $C_{18:0}$ ceramide; $C_{24:1}$, $C_{24:1}$ ceramide) or ceramide analogues (S16, *N*-palmitoyl serinol). $N > 5$; p value for difference between controls and FB1- or GW4869-treated cells, $^{**}p < 0.01$, and for difference between inhibitor-treated cells and those with $C_{16:0}$ ceramide, S16, or $C_{24:1}$ ceramide exogenously added, $^{*}p < 0.05$, $^{**}p < 0.01$. There is no significant difference between FB1- or GW4869-treated cells and those given exogenous $C_{18:0}$ ceramide.

antibody. In addition, reduction of ceramide levels led to redistribution of aPKC as well as residual ceramide to cytosolic vesicles (Figure 3, E and F), the origin of which remains to be determined. We assumed that the major obstacle to visualizing a complete distribution of ceramide came from lack of antibodies recognizing distinct ceramide species.

To achieve a more accurate signal distribution of distinct ceramide species and their colocalization with aPKC, we generated

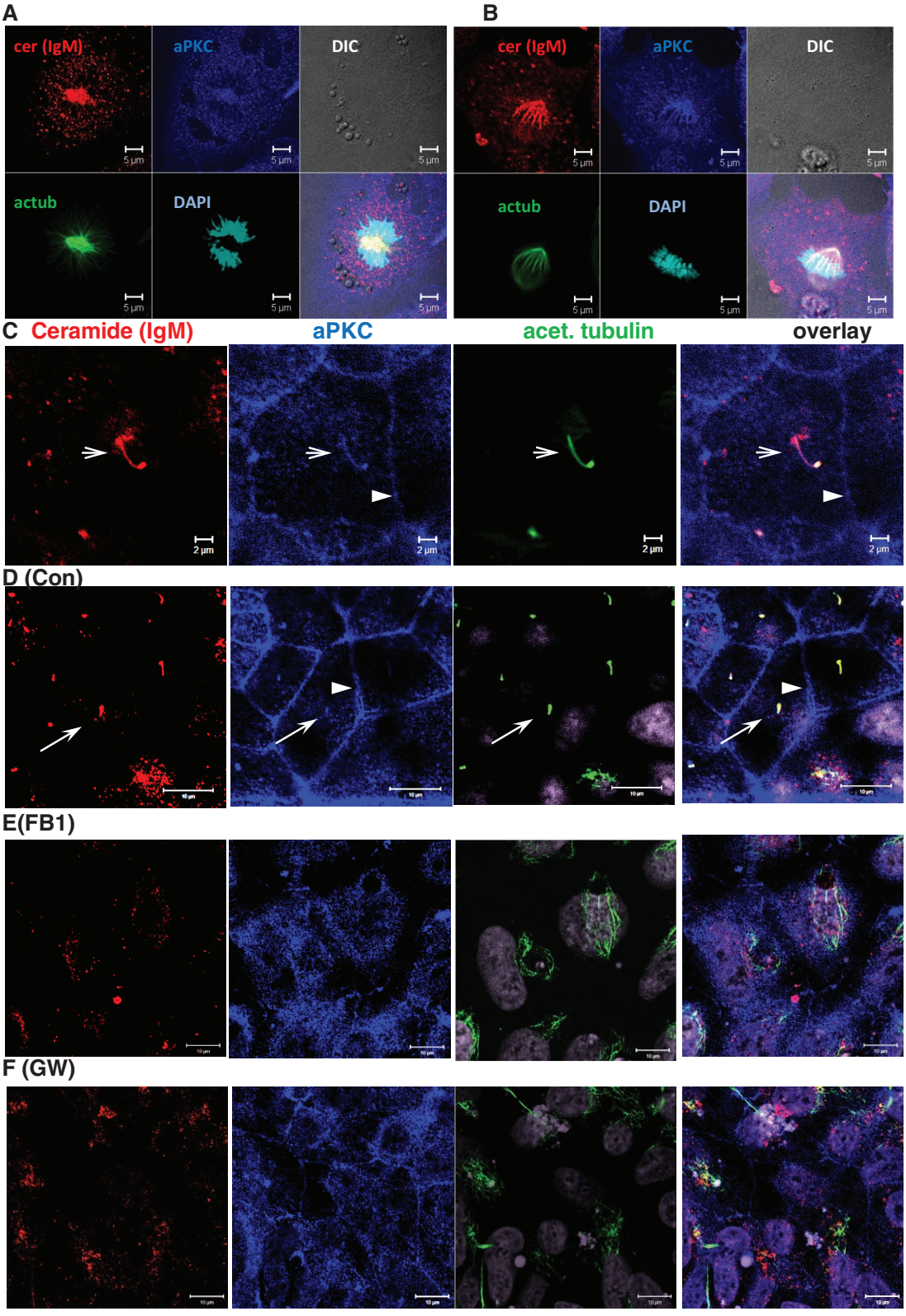

FIGURE 3: Ceramide depletion leads to translocation of aPKC from the primary cilium and the apicolateral cell membrane to the cytosol. NPs were analyzed using immunocytochemistry with anti-ceramide mouse IgM (red) and antibodies against acetylated tubulin (mouse IgG, green) and aPKC (C20, rabbit IgG, blue). (A, B) Mitotic cells. Note colocalization of ceramide with mitotic spindle. Bar, 5 μm. (C) Interphase (arrow points at primary cilium). 4′,6-Diamidino-2-phenylindole (DAPI) staining is pseudocolored in gray. Bar, 2 μm. (D–F) NPs differentiated from control (D) and FB1- (E) and GW4869-treated (F) human ES cells, followed by immunocytochemistry using antibodies as described for (A–C). aPKC is colocalized with the primary cilium (arrow) and the apicolateral cell membrane (arrowhead) of control cells (D). Colocalization is lost when cells are depleted of ceramide by treatment with FB1 (E) or GW4869 (F). Bars, 10 μm.

antibodies with high affinity toward either $C_{16:0}$ or $C_{24:0}$ ceramide. In addition to using $C_{16:0}$ or $C_{24:0}$ ceramide as separate antigens for immunization, we increased the antibody specificity by removing the $C_{24:0}$ ceramide and $C_{16:0}$ ceramide epitope–binding antibodies from the anti-$C_{16:0}$ and $C_{24:0}$ ceramide immunoglobulin G (IgG) fraction, respectively (see *Materials and Methods*). An enzyme-linked immunosorbent assay (ELISA)–based assay showed that the $C_{16:0}$ ceramide antibody fraction (termed anti-C16) and anti-ceramide IgM (MAS0014) mostly recognized $C_{16:0}$, whereas reactivity with $C_{24:0}$ ceramide was significantly reduced (Supplemental Table S1). ELISA also showed that anti-C24 recognized both $C_{24:0}$ and $C_{24:1}$ ceramide, whereas affinity to $C_{16:0}$ ceramide was almost negligible. Other sphingolipids, such as sphingomyelin, were not recognized by the anti-ceramide rabbit IgG or anti-ceramide IgM, as shown previously (Cowart *et al*., 2002; Krishnamurthy *et al*., 2007a).

Double labeling with anti-ceramide IgM showed colocalization with anti-C16 at primary cilia, indicating that both anti-ceramide IgM and anti-C16 could be used for labeling of apical ceramide (Supplemental Figure S7A). Anti-ceramide IgM in combination with anti-C24 showed that the signals for the two antibodies colocalized with acetylated tubulin at primary cilia in the apical plane (arrow in Figure 4A). However, only anti-C24 showed signals at the apicolateral cell membrane of NPs (arrow in Figure 4B), whereas anti-ceramide IgM or anti-C16 did not label the apicolateral cell membrane. On the basis of these observations, we concluded that the apicolateral cell membrane of NPs is specifically enriched with $C_{24:0}$ or $C_{24:1}$ but not $C_{16:0}$ ceramide, whereas primary cilia contained both $C_{16:0}$ and $C_{24:0/24:1}$ ceramide. Figure 4, C and D, shows that inhibition of ceramide generation with FB1 or GW4869 led to loss of anti-C24 labeling at the apicolateral cell membrane and reduction of anti-C24 and anti-C16 labeling in the apical region, concurrent with compromised ciliogenesis. The anti-C24 signal in the apicolateral membrane was restored when FB1-treated cells were incubated with $C_{24:1}$ ceramide (Supplemental Figure S7B), consistent with the ceramide specificity of anti-C24 and sphingolipidomics analysis showing that ceramide-depleted cells took up exogenous $C_{24:1}$ ceramide (Supplemental Figure S6A). There was some labeling of primary cilia detected with anti-ceramide IgM (arrow in Supplemental Figure S7B), which most likely indicated that a very small portion of $C_{16:0}$ ceramide either resided in FB1-treated cells or was generated from exogenous $C_{24:1}$ ceramide, which was also found with the lipidomics analysis (Supplemental Figure S6A). Based on the observation that FB1 and GW4869 treatment led to loss of $C_{24:0}$ and $C_{24:1}$ ceramide and aPKC labeling at the apicolateral membrane, our data indicated that the distribution of aPKC to the apicolateral cell membrane is likely mediated by very long chain ceramide. Further, our results suggest that loss of membrane sequestration due to ceramide depletion or reduction leads to translocation of aPKC to the cytosol.

Ceramide depletion leads to translocation and proteolytic activation of aPKC in the cytosol

To test for cytosolic translocation of aPKC by ceramide depletion, we performed a subcellular fractionation assay using differential centrifugation of NPs treated with FB1 or GW4869 and compared the distribution of aPKC with control cells. Figure 5A and Supplemental Figure S8 show that this treatment led to elevation of the 72-kDa, full-length aPKC in the cytosol and the appearance of a 65-kDa band, indicating proteolytic processing of aPKC. Of most interest, two cytosolic bands at 55 and 45 kDa were phosphorylated (Figure 5A and Supplemental Figure S8B), although the total intensity of these bands was either decreased (55 kDa) or unchanged (45 kDa). This result suggests that cytosolic translocation of aPKC was concurrent with proteolytic processing and enhanced phosphorylation of the 55- and 45-kDa isoforms of aPKC. There are more than four proteolytically processed isoforms of aPKC. Two of these isoforms (55 and 45 kDa) are cytosolic fragments of aPKC (aPKCcat) that are activated by phosphorylation (Smith *et al*., 2000, 2003; Smith and Smith, 2002; Bougie *et al*., 2012). Because the antibody used to detect total aPKC was raised against a peptide located at the C-terminus (see *Materials and Methods*), it is likely that the proteolytic processing occurred at the N-terminus. Alternatively, the low abundance of the 55-kDa band (Figure 5A and Supplemental Figure S8A) may also indicate additional processing at the C-terminus, resulting in removal of the epitope. Whereas the cytosolic elevation of the 72- and 65-kDa isoforms was similar in FB1- and GW4869-treated cells, reduction of these two aPKC isoforms in the membrane fraction was visible after incubation with FB1 but less pronounced upon GW4869 treatment (Figure 5A, middle). However, when considering the ratio of the cytosolic to membrane-bound aPKC isoforms, it is clear that this is tremendously enhanced in both FB1 and GW4869 cells, indicating that the protein levels of membrane-bound and cytosolic aPKC are in dynamic equilibrium, which is shifted to the cytosol by ceramide depletion. In summary, our data suggest that in NPs, ceramide depletion leads to loss of membrane sequestration of aPKC to the apicolateral cell membrane and generation of aPKCcat in the cytosol.

Because ceramide depletion led to translocation and activation of aPKC in the cytosol concurrent with loss of ciliogenesis, we next tested whether supplementation with exogenous ceramide restored the membrane distribution of aPKC. Supplemental Figure 9, A–C, shows that incubation of FB1-treated NPs with $C_{16:0}$ ceramide resulted in intense labeling of ceramide in vesicles that partially colocalized with aPKC (arrow in Supplemental Figure 9C) but it did not restore the cell membrane distribution of aPKC (Supplemental Figure S9, A and B, shows controls and FB1-treated cells, respectively). In contrast, $C_{24:1}$ ceramide restored the distribution of aPKC to the apicolateral cell membrane (Supplemental Figure S9D; arrow points at membrane, arrowhead at cilium). Consistent with this result, $C_{24:1}$ ceramide was more effective than $C_{16:0}$ ceramide in restoring ciliogenesis in ceramide-depleted cells (Figure 2C).

On the basis of the hypothesis that cytosolic translocation and activation of aPKCcat led to impaired ciliogenesis, we tested whether inhibition of aPKC would rescue primary cilia in ceramide-depleted cells. Figure 5B shows that incubation with PZI (a pseudosubstrate inhibitor of aPKC) or Go6983 (a pharmacological aPKC inhibitor) restored ciliogenesis in FB1-treated NPs. Similar results were obtained with GW4869-treated NPs in combination with PZI and Go6983 (unpublished data). These data are consistent with the hypothesis that ceramide-mediated aPKC sequestration prevented its activation and stabilized primary cilia.

Ceramide-mediated inhibition of HDAC6 promotes ciliogenesis and neural process formation

In our previous study, we found that in ceramide-depleted MDCK cells, primary cilia were rescued by trichostatin (TSA), an inhibitor of histone deacetylases (HDACs; He *et al*., 2012). We tested whether TSA could also restore primary cilium formation in ceramide-depleted NPs. TSA, however, had to be precluded from further experiments because of its toxicity to human ES cell–derived NPs (unpublished data). Therefore we used tubacin, an inhibitor specific for HDAC6. Figure 5B shows that tubacin, similar to aPKC inhibitors, partially restored ciliogenesis in FB1- or GW4869-treated cells, suggesting that ceramide promoted ciliogenesis by preventing activation of HDAC6.

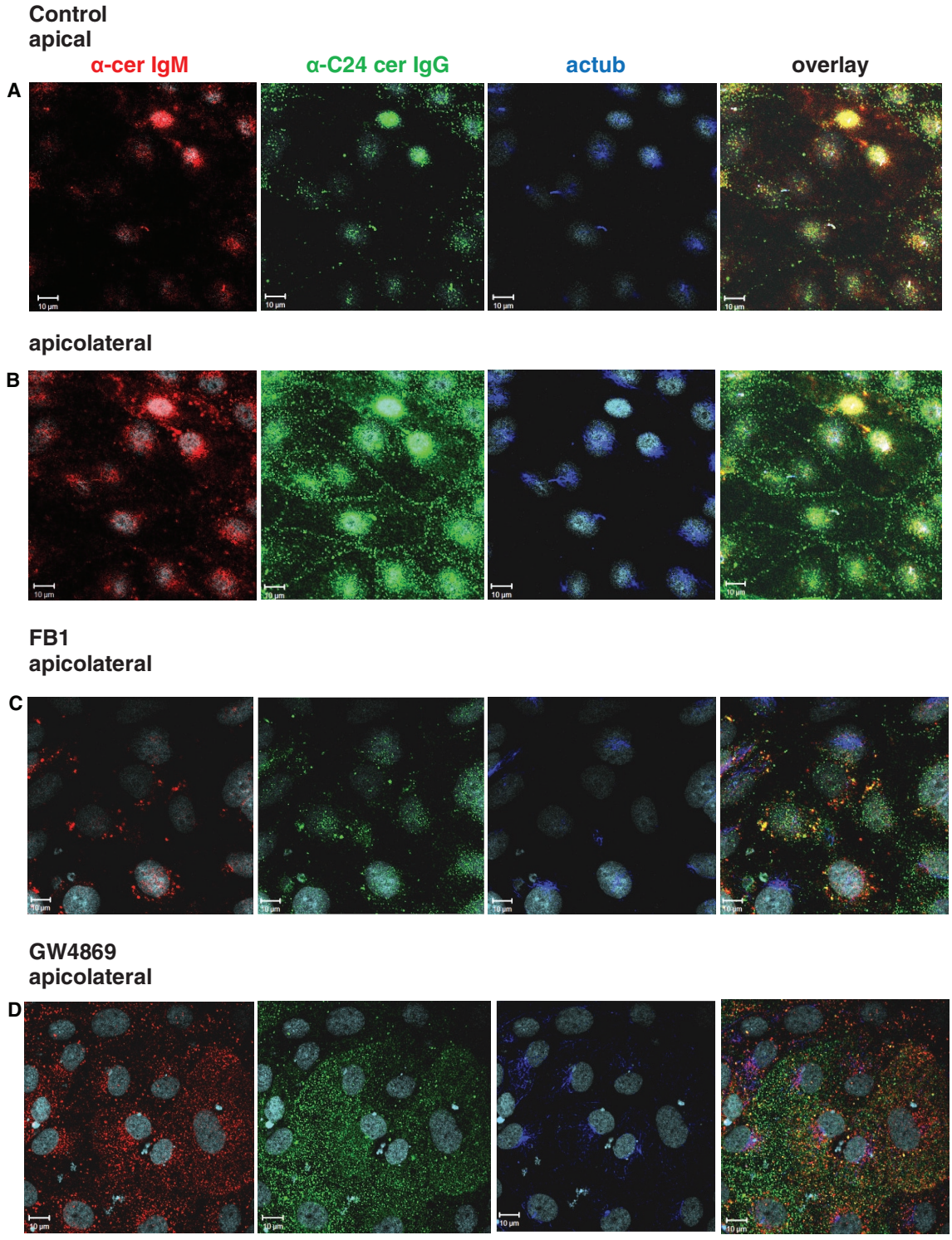

FIGURE 4: $C_{16:0}$ ceramide is localized at primary cilia, whereas $C_{24:0/24:1}$ ceramide is at primary cilia and the apicolateral cell membrane. Neural differentiation was performed in the presence or absence of FB1 or GW4869, followed by immunocytochemistry using antibodies against $C_{16:0}$ ceramide (anti-cerIgM) or $C_{24:0/C24:1}$ ceramide (anti-C24). DAPI staining is pseudocolored in gray, anti-ceramide IgM in red, anti-C24 ceramide IgG in green, and acetylated tubulin in blue. (A) Control, apical plane (arrow points at colocalization of anti-cerIgM, anti-C24, and anti-acetylated tubulin antibodies at primary cilia). (B) Control, apicolateral plane (arrow points at apicolateral cell membrane). (C) FB1-treated cells. (D) GW4869-treated cells. Bars, 10 μm.

On the basis of the observation that inhibition of HDAC6 or aPKC restored ciliogenesis in ceramide-depleted cells, we next tested the functional involvement of factors that mediate activation or inactivation of HDAC6 by aPKC. Previous studies showed that aPKC phosphorylates and activates Aurora A kinase (AurA), and AurA activates HDAC6, which in turn leads to cilium retraction and cell cycle reentry (Pugacheva *et al.*, 2007; Loktev *et al.*, 2008; Valenzuela-Fernandez *et al.*, 2008; Cao *et al.*, 2009; Mori *et al.*, 2009; Yamada *et al.*, 2010;

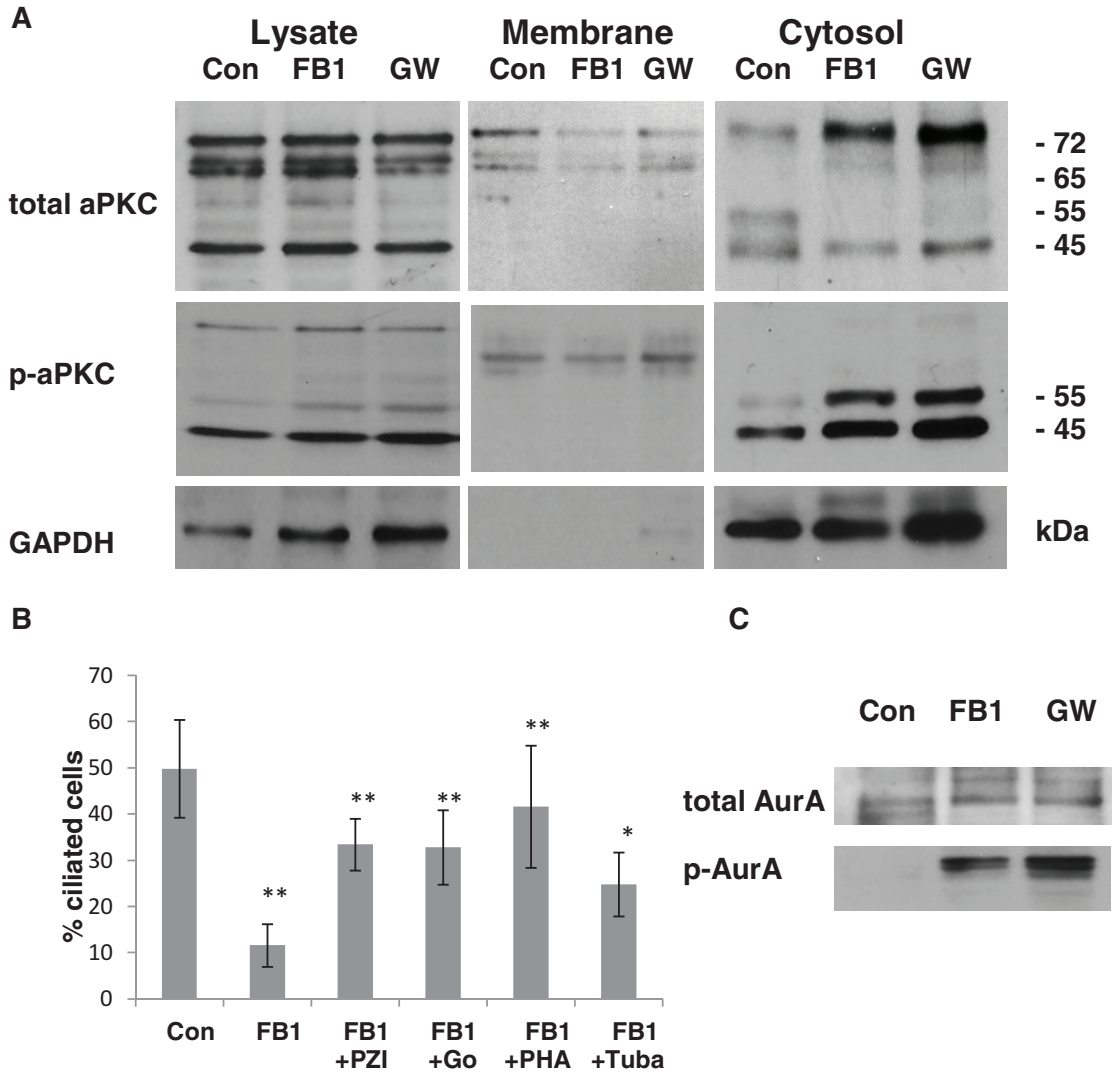

FIGURE 5: In ceramide-depleted cells, activation of cytosolic aPKC reduces ciliogenesis, whereas inhibition of HDAC6 and AurA rescues cilia. (A) Control and FB1- or GW4869-treated NPs were subjected to subcellular fractionation using differential centrifugation. The cytosolic fraction of ceramide-depleted cells contains a phosphorylated, 55-kDa isoform of aPKC (aPKCcat). In addition, there are 65- and 45-kDa isoforms, the latter of which is phosphorylated but it is also present in control cells. (B) Inhibition of aPKC with pseudo substrate inhibitor peptide of aPKC (PZI) or Go6983 (Go), or AurA and HDAC6 inhibition with PHA-680632 (PHA) and tubacin (Tuba), can partially rescue ciliogenesis in FB1-treated NPs. $N \geq 5$, $^{*}p < 0.05$ or $^{**}p < 0.01$ for comparison of treated cells with control. (C) Ceramide depletion leads to enhanced phosphorylation of AurA in the cytosolic fraction.

Gradilone *et al.*, 2013). Accordingly, we hypothesized that inhibition of aPKC (or inaccessibility of AurA as its substrate) would prevent activation of HDAC6 and stabilize primary cilia in the presence of ceramide. Because we assumed that ceramide sequestered aPKC to the apicolateral cell membrane, we tested whether translocation of aPKC to the cytosol would activate AurA in ceramide-depleted cells. Figure 5C shows that treatment of NPs with FB1 or GW4869 indeed induced AurA activation, as determined by the presence of phosphorylated AurA in the cytosolic fraction. Therefore membrane sequestration of aPKC by binding to ceramide may prevent activation of AurA and, in turn, HDAC6-mediated retraction of primary cilia. Consistent with this hypothesis, AurA inhibition with PHA-680632 restored ciliogenesis in ceramide-depleted cells (Figure 5B).

Inhibition of AurA halts NP self-renewal and promotes asymmetric cell division and neuronal differentiation (Lee *et al.*, 2006, 2012; Kim and Hirth, 2009; Reichert, 2011). Further, inhibition of HDAC6 is neuroprotective by stabilizing neuronal processes (Butler *et al.*, 2010; Govindarajan *et al.*, 2013; Xiong *et al.*, 2013). Because our data indicated that ceramide—in particular, $C_{24:1}$ ceramide—may prevent AurA activation by membrane sequestration of aPKC, we tested whether $C_{24:1}$ ceramide may also promote neural process formation. Figure 6, A and B, shows that in FB1-treated NPs, addition of $C_{24:1}$ ceramide to the medium led to an increased number of neural rosettes. In addition, after just 4 d of incubation, $C_{24:1}$ ceramide induced the formation of tremendously elongated (>200 µm) processes and NP cell complexes with the morphology of neural tube-like and columnar structures (Figure 6, C–E). These structures showed a polarized distribution of acetylated tubulin to primary cilia formed at high density on the presumptive "apical" side and neural processes on the "basal" side (Figure 6E; arrow points at primary cilia).

In addition to acetylated tubulin, neural processes expressed Map-2, which is a marker for mature neurons (Figure 7A).

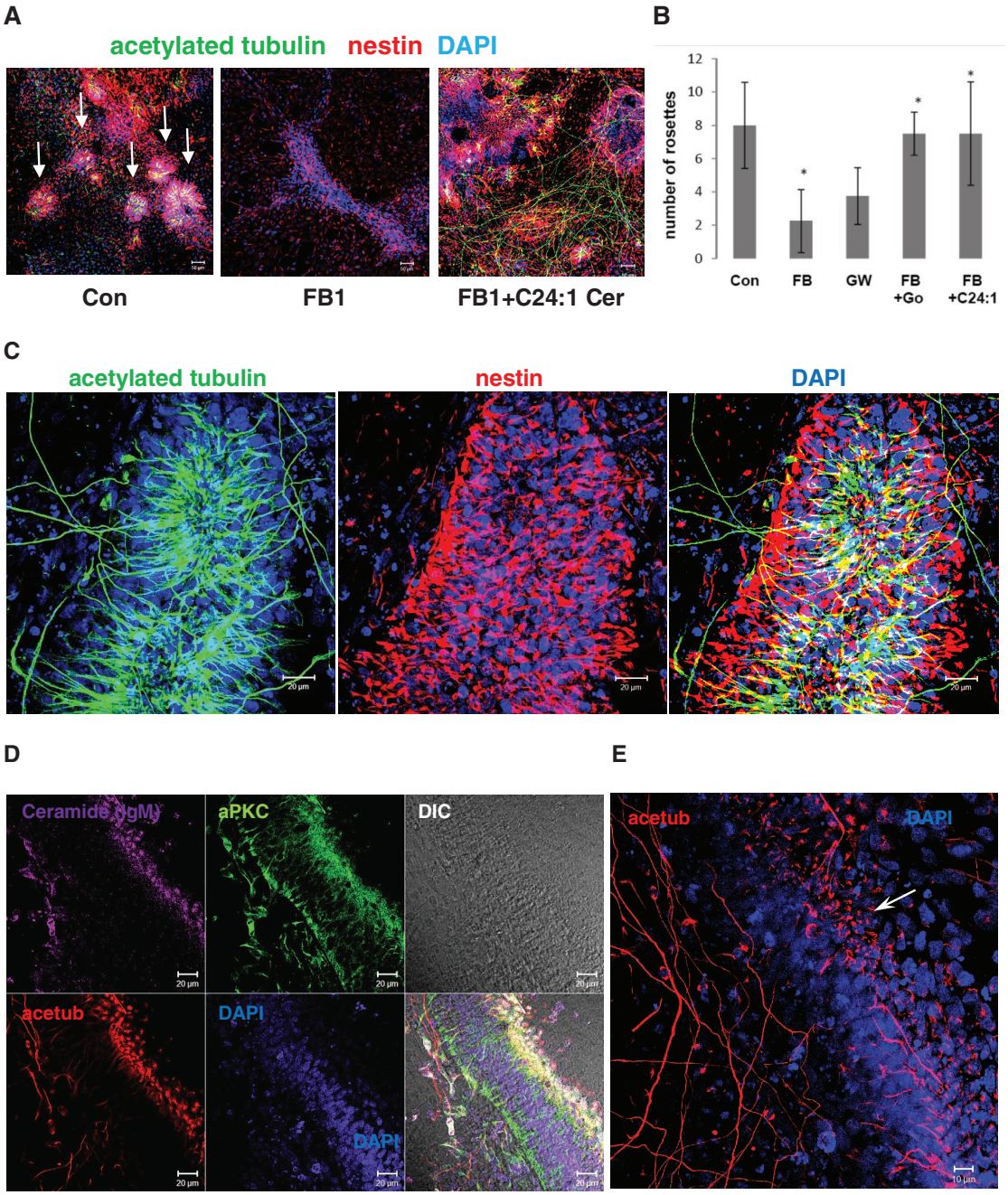

FIGURE 6: $C_{24:1}$ ceramide restores NP rosettes in ceramide-depleted cells. Human ES cells were differentiated for 5 d in the presence of 20 μM FB1 with or without 2 μM $C_{24:1}$ ceramide, followed by immunocytochemistry for acetylated tubulin (mouse or rabbit IgG), aPKC (rabbit IgG), ceramide (mouse IgM), or nestin (mouse IgG). A. Formation of neural rosettes (arrows) is severely reduced in ceramide-depleted NPs. (B) Treatment with $C_{24:1}$ ceramide restores the number of NP rosettes (>100 μm diameter) similar to the effect of aPKC inhibition with Go6983. $N = 3$, $p < 0.05$ for comparison of FB1-treated and $C_{24:1}$ ceramide–treated cells. (C–E) $C_{24:1}$ ceramide treatment promotes formation of acetylated tubulin–labeled processes and polarized neural tube–like structures (arrow in E points at primary cilia at apical side). Bars, 50 μm (A), 20 μm (C, D), and 10 μm (E).

$C_{24:1}$ ceramide–induced neuronal process formation was also observed with human iPS cells treated in the same way as human ES cells (Figure 7, B–D). Taken together, these data suggest not only that is ceramide—in particular very long chain $C_{24:1}$ ceramide—critical for the regulation of ciliogenesis, but it also promotes neural process formation of differentiating human ES and iPS cells.

DISCUSSION

Differentiation of ES cells crucially relies on growth factor receptors that are highly expressed on primary cilia. Human ES cells were described as generating primary cilia, although this study used only undifferentiated ES cells (Kiprilov *et al.*, 2008). In the present study, we show that NPs differentiated from human ES cells develop primary cilia and that ciliogenesis is regulated by ceramide,

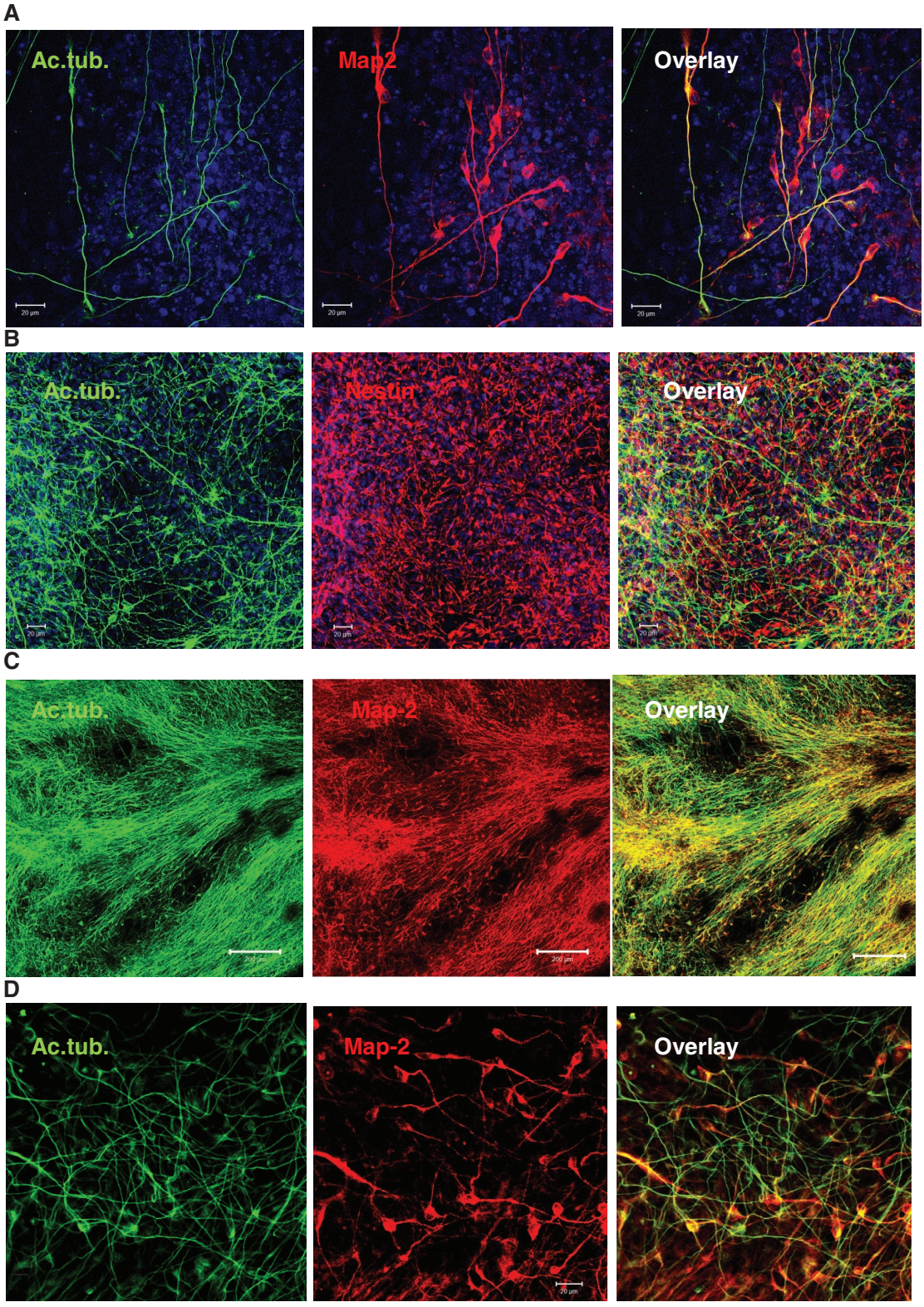

FIGURE 7: $C_{24:1}$ ceramide promotes neural process formation in human ES and iPS cells. Human ES or iPS cells were treated as described in the legend to Figure 6. (A) Colocalization of acetylated tubulin (green) and Map-2 (red) shows that many processes originate in neural progenitors or differentiated neurons. (B–D) Acetylated tubulin–labeled processes and nestin-labeled NPs are also visible in iPS cells that were differentiated following the protocol used for human ES cells. Neural processes of $C_{24:1}$ ceramide–treated iPS cells are elongated (>200 μm) and colabeled for Map-2. Bars, 20 μm (A, B, D), 200 μm (C).

a sphingolipid we previously found to be elevated during ES cell differentiation toward NPs (Bieberich *et al.*, 2003; Wang *et al.*, 2008). Of importance, ciliogenesis in these cells was part of a neural differentiation process initiated by growth factor withdrawal but without the addition of retinoic acid that is often used to accelerate neuronal differentiation.

There is growing evidence that the function of ceramide critically depends on its intracellular compartmentalization, such as the ACEC in polarized MDCK cells (Wang *et al.*, 2009a; He *et al.*, 2012). The discovery of the ACEC was possible because we used highly purified and specific rabbit polyclonal ceramide antibodies prepared in our laboratory (Krishnamurthy *et al.*, 2007a). Additional purification steps using ceramide vesicles further enhanced the specificity of these antibodies. An antibody designated "anti-C16" shows high binding affinity to long-chain $C_{16:0}$ ceramide but not to very long chain $C_{24:0}$ or $C_{24:1}$ ceramide (structures in Supplemental Figure S1). A second antibody dubbed "anti-C24" binds well to $C_{24:0}$ and $C_{24:1}$ ceramide but less well to $C_{16:0/18:0}$ ceramide. A third antibody used in our experiments was the commercially available anti-ceramide mouse IgM, which showed affinity to ceramide species that were also recognized by anti-C16. Therefore the specificity of the commercial antibody resembled that of the anti-C16, whereas the anti-C24 allowed for the novel visualization of very long chain ceramide.

The need for visualization of different ceramide species comes from our lipidomics data showing that elevation of ceramide during neural differentiation of human ES cells is mainly confined to $C_{16:0}$ and $C_{24:1}$ ceramides (Figure 2A and Supplemental Figure S6). Consistent with our previous studies and the observation that anti-C16 and anti-ceramide IgM detected ceramide at the cilium base in ES cell–derived NPs, $C_{16:0}$ ceramide likely partakes in a ciliogenic lipid–protein complex with aPKC. This assumption is supported by the results of immunocytochemistry showing that aPKC colocalizes with ceramide at the cilium base and the cilium itself (Figure 3C). In NP rosettes with apicobasal polarity, aPKC is also distributed to the apicolateral cell membrane (Figure 3, C and D). Most strikingly, anti-C24 detects ceramide in this region as well (Figure 4B). Therefore we conclude that a second, very long chain ceramide–aPKC complex is present at the apicolateral cell membrane, the composition and function of which may differ from that of the complex at the cilium base.

To test the function of various ceramide species for ciliogenesis in human ES cell–derived NPs, we first reduced the level of ceramide by incubation with the ceramide synthase inhibitor FB1 or the nSMase inhibitor GW4869 and then exogenously added distinct ceramide species to the medium. This approach was successful in many studies on the function of ceramide and was also used in our previous studies on ciliogenesis (Chalfant *et al.*, 2001; Ogretmen *et al.*, 2002; Sultan *et al.*, 2006; Wang *et al.*, 2009a; He *et al.*, 2012). As anticipated, FB1 significantly reduced cilium formation. GW4869, which has not been used before in this context, also compromised ciliogenesis, suggesting that ceramide generated by de novo synthesis or sphingomyelin degradation by nSMase2 is important for cilium formation. It should be noted that GW4869 can inhibit other nSMases as well. However, nSMase1 (Smpd2) and nSMase3 (Smpd4) are predominantly expressed in kidney and heart or skeletal muscle, respectively, whereas nSMase2 (Smpd3) is the main nSMase in neural cells (Mizutani *et al.*, 2001; Krut *et al.*, 2006; Wu *et al.*, 2010a; Clarke *et al.*, 2011). A mitochondrial nSMase (Smpd5) has also been described in mammalian cells, although it is less likely to affect sphingolipid metabolism in the apicolateral membrane or at primary cilia (Wu *et al.*, 2010b). Therefore we assume that the effect of GW4869 on ciliogenesis in NPs is mostly due to inhibition of nSMase2.

In ceramide-depleted NPs, ciliogenesis was restored by the ceramide species most increased during NP differentiation from ES cells—$C_{16:0}$ and $C_{24:1}$ ceramides. Consistent with this result, the ceramide analogue S16 (*N*-palmitoyl serinol) restored ciliogenesis to an extent similar to that of C_{16} ceramide. A sphingolipidomics analysis of ceramide-depleted cells treated with exogenous $C_{24:1}$ ceramide clearly showed that ceramide was taken up by the cells but was not converted to glycosphingolipids. This result and the rescue effect of S16 argue against the possibility that derivatives of ceramide such as glucosylceramide, galactosylceramide, or sphingomyelin are responsible for the restoration of ciliogenesis.

Because ceramide colocalized with aPKC in primary cilia, we tested whether the interaction between ceramide and aPKC is important for ciliogenesis. We incubated control or ceramide-depleted NPs with two aPKC inhibitors—pseudosubstrate inhibitor peptide of PKCzeta (PZI) and Go6983—since these inhibitors prevented ciliogenesis in MDCK cells (Wang *et al.*, 2009a). To our surprise, aPKC inhibition did not prevent cilium formation, but it did restore ciliogenesis in ceramide-depleted NPs. This result suggested that ciliogenesis in NPs was driven by ceramide-mediated inhibition or sequestration of aPKC. It was previously shown that aPKC can be activated by proteolytic release and phosphorylation of the catalytic domain (aPKCcat) in the cytosol (Smith *et al.*, 2000, 2003; Garin *et al.*, 2007). Consistent with the assumption that ceramide depletion may trigger cytosolic translocation and proteolytic activation of aPKC, we found that incubation of NPs with FB1 or GW4869 led to the release of proteolytically processed isoforms of aPKC (designated aPKCcat) from the apicolateral cell membrane and appearance of aPKCcat in the cytosolic fraction (Figures 3, E and F, and 5A). Cytosolic aPKCcat was phosphorylated, further supporting the idea that cytosolic isoforms are activated by ceramide depletion. At this point, it remains to elucidate the sequence in which the aPKC processing occurs. Membrane release, proteolysis, and phosphorylation are triggered by ceramide depletion, but the exact sequence of these steps and their regulation by different ceramide species is unknown. Immunocytochemistry showed that incubation of FB1-treated NPs with $C_{24:1}$ ceramide but not C_{16} ceramide restored localization of aPKC to the apicolateral cell membrane, although the two ceramide species restored ciliogenesis. These results indicate that the function of $C_{16:0}$ ceramide for ciliogenesis may be different from that of $C_{24:1}$ ceramide. Taken together, our data suggest that the function of the proposed $C_{24:1}$ ceramide–aPKC complex at the apicolateral cell membrane is to prevent cytosolic translocation and activation of aPKCcat. Further, our results indicate that preventing aPKC activation by $C_{24:1}$ ceramide-mediated sequestration is likely to promote ciliogenesis.

To elucidate the mechanism by which aPKC sequestration to the apicolateral cell membrane promotes primary cilia formation, we first tested whether inhibition of one of its downstream targets, HDAC6, restores ciliogenesis. HDAC6 is activated by an aPKC-to-AurA cell signaling pathway and induces retraction of primary cilia by deacetylation of tubulin (Pugacheva *et al.*, 2007; Mori *et al.*, 2009; Yamada *et al.*, 2010). We previously showed that inhibition of HDAC6 restores ciliogenesis in MDCK cells (He *et al.*, 2012). Consistent with our data from MDCK cells, inhibition of HDAC6 with tubacin rescued ciliogenesis in FB1-treated NPs, suggesting that ceramide prevented activation of HDAC6 and therefore destabilization of microtubules. Ceramide depletion would thus lead to HDAC6-mediated deacetylation and retraction of primary cilia. In agreement with previous studies showing that aPKC can activate AurA, we

found that in FB1- or GW4869-treated cells, AurA is phosphorylated, indicative of its activation (Mori *et al.*, 2009; Yamada *et al.*, 2010). Moreover, the AurA inhibitor PHA-680632 restored primary cilia in FB1-treated NPs, further supporting the hypothesis that reduced ciliogenesis in ceramide-depleted cells is mediated by AurA activation. Because it was shown that AurA activates HDAC6, our data suggest that ceramide-mediated sequestration of aPKC sustains ciliogenesis by preventing aPKCcat-to-AurA-to-HDAC6 activation (Pugacheva *et al.*, 2007).

AurA activity has been found to be essential for ES cell renewal, whereas its down-regulation results in stem cell differentiation (Kim and Hirth, 2009; Lee *et al.*, 2012). Further, activation of AurA is required for progression of the cell cycle from the G2 phase to mitosis, concurrent with retraction of primary cilia (Persico *et al.*, 2010; Toughiri *et al.*, 2013). Finally, inhibition of AurA has been shown to stabilize primary cilia, which are known to be endowed with numerous receptors for growth factors and morphogens, including those important for neural differentiation (Pugacheva *et al.*, 2007; Spassky *et al.*, 2008; Han and Alvarez-Buylla, 2010; Amador-Arjona *et al.*, 2011; Ruat *et al.*, 2012). Therefore we assumed that ceramide-mediated sequestration of aPKC to the apicolateral cell membrane not only will sustain ciliogenesis, but it will also coincide with neural differentiation of human ES cells. Consistent with this assumption, addition of $C_{24:1}$ ceramide to FB1-treated ES cells increased the number of neural rosettes and even induced the formation of long processes in NPs, mimicking the morphology of neural tube–like structures in vitro (Figure 6). Based on the observation that FB1-treated cells did not show reduction of the NP marker Sox1 (Supplemental Figure S4D), it is unlikely that ceramide depletion disturbed neural differentiation per se due to loss of cilia. This assumption is consistent with previous reports that in mouse embryos or differentiating mouse ES cells, loss of primary cilia does not affect neural induction (Hunkapiller *et al.*, 2011). In addition to regulating ciliogenesis, ceramide may also be critical for neural morphogenesis such as NP rosette and neural process formation. This may not be surprising, since acetylation of tubulin is known to stabilize neuronal processes, and therefore inhibition of HDAC6 by ceramide may serve a dual purpose by promoting ciliogenesis as well as neural process formation (Butler *et al.*, 2010; Govindarajan *et al.*, 2013). It should be noted that neural processes were labeled for Map-2, which is a clear indication of neuronal differentiation in $C_{24:1}$ ceramide–treated human ES and iPS cells (Supplemental Figure S9).

A potential source for endogenous $C_{24:1}$ ceramide is $C_{24:1}$ sphingomyelin converted to ceramide by nSMase2 at the plasma membrane (Cowart *et al.*, 2006; Sauane *et al.*, 2010; Qin *et al.*, 2012). Consistent with this assumption, we found that 1) $C_{24:1}$ sphingomyelin is a major sphingomyelin species in human ES cell–derived NPs (Supplemental Figure S6C), 2) anti-C24 labels ceramide at primary cilia and the apicolateral cell membrane (Figure 4, A and B), and 3) the nSMase inhibitor GW4869 prevents ciliogenesis (Figure 2C). The importance of nSMase2 for ciliogenesis during neural development is supported by studies showing that nSMase2 deficiency leads to dwarfism and abnormal development of endocrine neurons in the hypothalamus (Aubin *et al.*, 2005; Stoffel *et al.*, 2007). However, these studies did not investigate the role of ceramide in primary cilia formation or neural stem cell differentiation. Taken together, our results suggest that nSMase2-derived $C_{24:1}$ ceramide forms attachment sites at the apicolateral cell membrane of NPs for sequestration of aPKC, which leads to reduced AurA and HDAC6 activation and, in turn, stabilization of primary cilia. This sequence of events may also promote neural process formation. Our study is the first to show that $C_{24:1}$ ceramide critically regulates primary cilium formation during neural stem cell differentiation and provides strong experimental evidence that very long chain ceramide is a vital factor for nervous system development.

MATERIALS AND METHODS

Reagents

Each experiment was performed with three different human ES cell lines obtained from various sources: BG01 (Bresagen, Adelaide, Australia), hOct4-GFP (Life Technologies, Carlsbad, CA), and H9 (Wicell, Madison, WI). Detection of primary cilia and ceramide was also performed with human iPS cells (GM23394) obtained from the Corriell Institute for Medical Research (Camden, NJ). Anti-ceramide antibodies were purchased from Sigma-Aldrich (St. Louis, MO; 15B4, mouse IgM) and Glycobiotech (Kuekels, Germany; MAS0020 and MAB0014, mouse IgM) or generated in our laboratory (anti-C_{16} ceramide rabbit IgG, anti-$C_{24/C24:1}$ ceramide rabbit IgG). Anti-PKCζ (C20, sc-216) was from Santa Cruz Biotechnology (Santa Cruz, CA). Anti–phospho-aurora A kinase (pAurA) rabbit IgG (2914S), anti-phospho-PKCζ/λ (Thr-410/403) rabbit IgG (9378P), and anti-acetylated tubulin rabbit IgG (3971) were from Cell Signaling Technology (Danvers, MA). Anti-PKCζ rabbit IgG (serum, P-0713), anti–AurA kinase mouse IgG (A1231), anti–glyceraldehyde-3-phosphate dehydrogenase mouse IgG, anti-acetylated tubulin mouse IgG, and trichostatin A were purchased from Sigma-Aldrich. Fumonisin B1 (FB1) and tubacin were from Enzo Life Sciences (Farmingdale, NY). Anti-HDAC6 mouse IgG (GTX 84377) was obtained from GeneTex (Irvine, CA). GW4869 was purchased from Cayman (Ann Arbor, MI), and PHA-680632 and Go6983 (S2911) were from Selleckchem.com (Houston, TX). Noggin and SB431542 were from R&D Systems (Minneapolis, MN). Cell culture media, nonessential amino acids (NEAA), GlutaMAX, and penicillin/streptomycin were from Corning Cellgro (Manassas, VA). KSR, bFGF, and Geltrex were from Life Technologies. Ceramide and other lipids were from Avanti Polar Lipids (Alabaster, AL). All reagents and solvents were of analytical quality.

Cultivation and neural differentiation of human ES and iPS cells

MEFs were inactivated by irradiation and then seeded on gelatin-coated tissue culture plates. After allowing for cell adherence, cells were cultivated overnight for conditioning in human ES cell (hESC) or iPS cell medium containing DMEM/F12, 20% KSR, 1% NEAA, 1% GlutaMAX, 1% penicillin/streptomycin, 0.1% 2-mercaptoethanol, and 8 ng/ml (iPS cells, 20–100 ng/ml) bFGF. About half of the MEF-conditioned medium (MEF-CM) was replaced with fresh hESC medium every day for up to a maximum of 7 d. Human ES and iPS cells were maintained on MEFs and then transitioned to feeder-free conditions by first preattaching feeder fibroblast on noncoated tissue culture dishes and then plating the nonattached ES cells on tissue culture dishes coated with Geltrex according to the manufacturer's (Life Technologies) protocol. To initiate NP differentiation, the human ES or iPS cells were subjected to three different protocols. Following the method developed by Swistowski *et al.* (2010), human ES cells were first cultivated as embryoid bodies in suspension and then plated as attached embryoid bodies, followed by dissociation and cultivation on Geltrex-coated NPs in N2-supplemented DMEM/F12 for 5 d. We also used the method developed by Chambers *et al.* (2009) by cultivating a human ES cell monolayer in the presence of two inhibitors of SMAD signaling—noggin and SB431542—followed by gradually adding N2-supplemented DMEM/F12 to 20%

KSR medium until reaching a final concentration of 5% KSR. Finally, we used a modified protocol by first growing human ES or iPS cells to 70% confluence and then changing the medium to mercaptoethanol and bFGF-free DMEM/F12 supplemented with 5% KSR, 1% NEAA, 1% GlutaMAX, and 1% penicillin/streptomycin as previously described (Dhara *et al.*, 2008; Dhara and Stice, 2008). To achieve >80% NP differentiation (as determined by the expression of nestin, Sox2, and Pax6), cells were incubated in 5% KSR medium for 5 d with daily changes of the medium. During the cultivation period, cells were also incubated with inhibitors for ceramide generation (20 µM FB1 or 10 µM GW4869), aPKC inhibitors (30 µM PZI or 2 µM Go6983), ceramide (2 µM C_{16}, C_{18}, C_{24}, or $C_{24:1}$ ceramide diluted from a 1000× stock in ethanol/2% dodecane) or combinations of these reagents. Tubacin (2 µM) or PHA-680632 (0.5 µM) was added only for the last 24–48 h of NP differentiation.

Lipid analysis

Total lipids were extracted from cells using a mixture of chloroform-methanol (2:1; vol/vol) and further analyzed by HPTLC as previously described (Bieberich *et al.*, 2003). In brief, the ceramide species were separated by HPTLC using the running solvent chloroform-methanol-acetic acid (95:5:0.5; vol/vol/vol). Individual bands were visualized by staining with either iodine or charring with 3% cupric acetate in 8% phosphoric acid. The amount of ceramide was quantified by comparing the sample bands to the staining intensity of standard ceramide using densitometry and ImageJ (National Institutes of Health, Bethesda, MD) analysis. Sphingolipidomics analysis by LC-MS/MS was performed at the lipidomics core facility of the Medical University of South Carolina, Charleston, SC (under the directorship of Jacek Bielawski). For HPTLC and LC-MS/MS analyses, the ceramide composition was normalized to lipid phosphate or protein as indicated in the figures.

Preparation and characterization of high-affinity C_{24} and $C_{24:1}$ ceramide antibodies

A C_{24} ceramide emulsion was prepared with keyhole limpet hemocyanin in phosphate-buffered saline (PBS) and Freund's complete adjuvant (Sigma-Aldrich) as described previously (Krishnamurthy *et al.*, 2007a). In brief, the emulsion was injected subcutaneously into rabbits, followed by booster doses using incomplete adjuvant. Serum was collected from blood and the immunoglobulin fraction precipitated using ammonium sulfate. The pellet was dissolved in PBS and the dialyzed retentate used for IgG purification by DEAE–Sepharose chromatography. The IgG fraction was preserved at –20°C after adding an equal volume of glycerol. The specificity of the antibody was tested against different ceramide species using ELISA assays (Supplemental Table S1). To attain the higher specificity toward $C_{24:0}$ and $C_{24:1}$ ceramides, the IgG preparation was absorbed using ceramide vesicles.

Briefly, $C_{18:0}$ ceramide, $C_{18:0}$ phosphatidyl choline; $C_{18:0}$ phosphatidyl serine, or sphingomyelin and cholesterol were mixed at a concentration of 0.15 mM each in an Eppendorf tube and then dried under nitrogen. Tris-HCl (0.05 M, pH 7.4) buffer containing 0.1 mM $MnCl_2$ was added to the dried mixtures and the solution sonicated. The solution was then centrifuged at 9000 × *g* for 20 min, and the pellet was washed with an equal volume of Tris-HCl (0.05 M, pH 7.4) containing 150 mM NaCl and centrifuged again. The supernatant was removed, and the vesicles were washed once with PBS and resuspended in 50 µl of PBS, followed by sonication for 30 min. To the vesicle suspension, 250 µl of the anti-C_{24} ceramide IgG was added and incubated overnight at 4°C. The absorbed IgG was centrifuged at 9000 × *g* for 15 min, and the specificity of the antibody assayed by ELISA against $C_{16:0}$, $C_{18:0}$, and $C_{24:0}$ ceramides at different antibody dilutions. The procedure was repeated one or two more times in order to achieve the desired specificity. The $C_{18:0}$ ceramide vesicles were more effective in neutralizing both $C_{16:0}$- and $C_{18:0}$ ceramide affinity compared with $C_{16:0}$ ceramide vesicles. The antibody was found to be equally active against $C_{24:0}$ and $C_{24:1}$ ceramides, whereas it did not show any activity toward any glycosphingolipid using immune-overlay assays. Anti-$C_{16:0}$ ceramide was prepared in a similar way using $C_{24:0}$ ceramide vesicles for removal of the $C_{24:0/24:1}$ ceramide–specific IgGs.

Immunocytochemistry and image analysis

Human ES cells were fixed with 4% paraformaldehyde (PFA)/PBS or 4% PFA/0.1% glutaraldehyde for 15 min at room temperature or 37°C to preserve tubulin polymers. Fixed cells were rinsed two times with PBS and then briefly permeabilized by incubation with 0.2% Triton X-100/PBS for 5 min at room temperature. Immunocytochemistry and image acquisition were performed as described previously (He *et al.*, 2012).

Subcellular fractionation

Human ES cells were differentiated to NPs with or without inhibitors of ceramide generation, scraped off, harvested by centrifugation, and then resuspended in 1 ml of HEPES–sucrose buffer (10 mM HEPES, 250 mM sucrose, 1 mM ethylene glycol tetraacetic acid, 1 mM EDTA, and 2 mM $MgCl_2$) supplemented with protease and phosphatase inhibitor cocktails (Sigma-Aldrich). The cell suspension was rendered hypotonic by adding an equal volume of water and then stored on ice for 30 min. Once cells appeared swollen, they were disrupted using a tight-fitting Teflon pestle attached to a Potter S homogenizer set to 600–1000 rpm. Cells were inspected under a microscope to ensure complete homogenization and then subjected to differential centrifugation as previously described (Krishnamurthy *et al.*, 2007b). After removal of cell debris, nuclei, mitochondria, and lysosomes, the pellet of the final centrifugation step (110,000 × *g* for 2 h) was designated "membrane fraction" and the supernatant "cytosolic fraction."

Statistics

Counting of cells with particular fluorescence signals for cilium formation or distribution of other antigens was performed by three individuals in a blinded assay using at least five fields on each section or slide from four independent samples with at least 50 cells in each field. Means and SD were determined for counts of single signals and the signal distributions analyzed using a two-tailed, equal-variance Student's *t* test, with $p < 0.05$ considered statistically significant.

ACKNOWLEDGMENTS

This work is funded by the National Science Foundation (NSF1121579) and in part by the Georgia Research Alliance Fund to E.B. G.W. is supported by a Scientist Development grant from the American Heart Association. We thank the imaging core facility (under the supervision of Ana McNeil and Paul McNeil) for help with confocal microscopy. In addition, we thank the sphingolipidomics core facility at the Medical University of South Carolina (under the supervision of Jacek Bielawski) for the LC-MS/MS analyses of sphingolipids. We are also grateful to the Institute of Molecular Medicine and Genetics (Director Lin Mei), Georgia Regents University, Augusta, GA, for institutional support.

REFERENCES

Amador-Arjona A, Elliott J, Miller A, Ginbey A, Pazour GJ, Enikolopov G, Roberts AJ, Terskikh AV (2011). Primary cilia regulate proliferation of amplifying progenitors in adult hippocampus: implications for learning and memory. J Neurosci 31, 9933–9944.

Aubin I *et al*. (2005). A deletion in the gene encoding sphingomyelin phosphodiesterase 3 (Smpd3) results in osteogenesis and dentinogenesis imperfecta in the mouse. Nat Genet 37, 803–805.

Bieberich E, Kawaguchi T, Yu RK (2000). N-acylated serinol is a novel ceramide mimic inducing apoptosis in neuroblastoma cells. J Biol Chem 275, 177–181.

Bieberich E, MacKinnon S, Silva J, Noggle S, Condie BG (2003). Regulation of cell death in mitotic neural progenitor cells by asymmetric distribution of prostate apoptosis response 4 (PAR-4) and simultaneous elevation of endogenous ceramide. J Cell Biol 162, 469–479.

Bougie JK, Cai D, Hastings M, Farah CA, Chen S, Fan X, McCamphill PK, Glanzman DL, Sossin WS (2012). Serotonin-induced cleavage of the atypical protein kinase C Apl III in *Aplysia*. J Neurosci 32, 14630–14640.

Butler KV, Kalin J, Brochier C, Vistoli G, Langley B, Kozikowski AP (2010). Rational design and simple chemistry yield a superior, neuroprotective HDAC6 inhibitor, tubastatin A. J Am Chem Soc 132, 10842–10846.

Cao M, Li G, Pan J (2009). Regulation of cilia assembly, disassembly, and length by protein phosphorylation. Methods Cell Biol 94, 333–346.

Chalfant CE, Ogretmen B, Galadari S, Kroesen BJ, Pettus BJ, Hannun YA (2001). FAS activation induces dephosphorylation of SR proteins; dependence on the de novo generation of ceramide and activation of protein phosphatase 1. J Biol Chem 276, 44848–44855.

Chambers SM, Fasano CA, Papapetrou EP, Tomishima M, Sadelain M, Studer L (2009). Highly efficient neural conversion of human ES and iPS cells by dual inhibition of SMAD signaling. Nat Biotechnol 27, 275–280.

Clarke CJ, Wu BX, Hannun YA (2011). The neutral sphingomyelinase family: identifying biochemical connections. Adv Enzyme Regul 51, 51–58.

Cowart LA, Okamoto Y, Lu X, Hannun YA (2006). Distinct roles for de novo versus hydrolytic pathways of sphingolipid biosynthesis in *Saccharomyces cerevisiae*. Biochem J 393, 733–740.

Cowart LA, Szulc Z, Bielawska A, Hannun YA (2002). Structural determinants of sphingolipid recognition by commercially available anti-ceramide antibodies. J Lipid Res 43, 2042–2048.

Desai K, Sullards MC, Allegood J, Wang E, Schmelz EM, Hartl M, Humpf HU, Liotta DC, Peng Q, Merrill AHJr (2002). Fumonisins and fumonisin analogs as inhibitors of ceramide synthase and inducers of apoptosis. Biochim Biophys Acta 1585, 188–192.

Dhara SK, Hasneen K, Machacek DW, Boyd NL, Rao RR, Stice SL (2008). Human neural progenitor cells derived from embryonic stem cells in feeder-free cultures. Differentiation 76, 454–464.

Dhara SK, Stice SL (2008). Neural differentiation of human embryonic stem cells. J Cell Biochem 105, 633–640.

Dobierzewska A, Shi L, Karakashian AA, Nikolova-Karakashian MN (2012). Interleukin 1beta regulation of FoxO1 protein content and localization: evidence for a novel ceramide-dependent mechanism. J Biol Chem 287, 44749–44760.

Garin G, Abe J, Mohan A, Lu W, Yan C, Newby AC, Rhaman A, Berk BC (2007). Flow antagonizes TNF-alpha signaling in endothelial cells by inhibiting caspase-dependent PKC zeta processing. Circ Res 101, 97–105.

Gerdes JM, Davis EE, Katsanis N (2009). The vertebrate primary cilium in development, homeostasis, and disease. Cell 137, 32–45.

Govindarajan N, Rao P, Burkhardt S, Sananbenesi F, Schluter OM, Bradke F, Lu J, Fischer A (2013). Reducing HDAC6 ameliorates cognitive deficits in a mouse model for Alzheimer's disease. EMBO Mol Med 5, 52–63.

Gradilone SA, Radtke BN, Bogert PS, Huang BQ, Gajdos GB, Larusso NF (2013). HDAC6 inhibition restores ciliary expression and decreases tumor growth. Cancer Res 73, 2259–2270.

Han YG, Alvarez-Buylla A (2010). Role of primary cilia in brain development and cancer. Curr Opin Neurobiol 20, 58–67.

He Q, Wang G, Dasgupta S, Dinkins M, Zhu G, Bieberich E (2012). Characterization of an apical ceramide-enriched compartment regulating ciliogenesis. Mol Biol Cell 23, 3156–3166.

Hunkapiller J, Singla V, Seol A, Reiter JF (2011). The ciliogenic protein Oral-Facial-Digital 1 regulates the neuronal differentiation of embryonic stem cells. Stem Cells Dev 20, 831–841.

Kim DW, Hirth F (2009). Genetic mechanisms regulating stem cell self-renewal and differentiation in the central nervous system of *Drosophila*. Cell Adh Migr 3, 402–411.

Kiprilov EN *et al*. (2008). Human embryonic stem cells in culture possess primary cilia with hedgehog signaling machinery. J Cell Biol 180, 897–904.

Komatsu Y, Mishina Y (2013). Establishment of left-right asymmetry in vertebrate development: the node in mouse embryos. Cell Mol Life Sci 70, 4659–4666.

Krishnamurthy K, Dasgupta S, Bieberich E (2007a). Development and characterization of a novel anti-ceramide antibody. J Lipid Res 48, 968–975.

Krishnamurthy K, Wang G, Silva J, Condie BG, Bieberich E (2007b). Ceramide regulates atypical PKCζ/λ-mediated cell polarity in primitive ectoderm cells: a novel function of sphingolipids in morphogenesis. J Biol Chem 282, 3379–3390.

Krut O, Wiegmann K, Kashkar H, Yazdanpanah B, Kronke M (2006). Novel tumor necrosis factor-responsive mammalian neutral sphingomyelinase-3 is a C-tail-anchored protein. J Biol Chem 281, 13784–13793.

Lee CY, Andersen RO, Cabernard C, Manning L, Tran KD, Lanskey MJ, Bashirullah A, Doe CQ (2006). *Drosophila* Aurora-A kinase inhibits neuroblast self-renewal by regulating aPKC/Numb cortical polarity and spindle orientation. Genes Dev 20, 3464–3474.

Lee DF *et al*. (2012). Regulation of embryonic and induced pluripotency by aurora kinase-p53 signaling. Cell Stem Cell 11, 179–194.

Loktev AV, Zhang Q, Beck JS, Searby CC, Scheetz TE, Bazan JF, Slusarski DC, Sheffield VC, Jackson PK, Nachury MV (2008). A BBSome subunit links ciliogenesis, microtubule stability, and acetylation. Dev Cell 15, 854–865.

Marasas WF *et al*. (2004). Fumonisins disrupt sphingolipid metabolism, folate transport, and neural tube development in embryo culture and in vivo: a potential risk factor for human neural tube defects among populations consuming fumonisin-contaminated maize. J Nutr 134, 711–716.

Marchesini N, Luberto C, Hannun YA (2003). Biochemical properties of mammalian neutral sphingomyelinase 2 and its role in sphingolipid metabolism. J Biol Chem 278, 13775–13783.

Mizutani Y, Tamiya-Koizumi K, Nakamura N, Kobayashi M, Hirabayashi Y, Yoshida S (2001). Nuclear localization of neutral sphingomyelinase 1: biochemical and immunocytochemical analyses. J Cell Sci 114, 3727–3736.

Mori D, Yamada M, Mimori-Kiyosue Y, Shirai Y, Suzuki A, Ohno S, Saya H, Wynshaw-Boris A, Hirotsune S (2009). An essential role of the aPKC-Aurora A-NDEL1 pathway in neurite elongation by modulation of microtubule dynamics. Nat Cell Biol 11, 1057–1068.

Ogretmen B, Pettus BJ, Rossi MJ, Wood R, Usta J, Szulc Z, Bielawska A, Obeid LM, Hannun YA (2002). Biochemical mechanisms of the generation of endogenous long chain ceramide in response to exogenous short chain ceramide in the A549 human lung adenocarcinoma cell line. Role for endogenous ceramide in mediating the action of exogenous ceramide. J Biol Chem 277, 12960–12969.

Pan J, Snell W (2007). The primary cilium: keeper of the key to cell division. Cell 129, 1255–1257.

Persico A, Cervigni RI, Barretta ML, Corda D, Colanzi A (2010). Golgi partitioning controls mitotic entry through Aurora-A kinase. Mol Biol Cell 21, 3708–3721.

Pruett ST, Bushnev A, Hagedorn K, Adiga M, Haynes CA, Sullards MC, Liotta DC, Merrill AHJr (2008). Biodiversity of sphingoid bases ("sphingosines") and related amino alcohols. J Lipid Res 49, 1621–1639.

Pugacheva EN, Jablonski SA, Hartman TR, Henske EP, Golemis EA (2007). HEF1-dependent Aurora A activation induces disassembly of the primary cilium. Cell 129, 1351–1363.

Qin J, Berdyshev E, Poirer C, Schwartz NB, Dawson G (2012). Neutral sphingomyelinase 2 deficiency increases hyaluronan synthesis by up-regulation of hyaluronan synthase 2 through decreased ceramide production and activation of Akt. J Biol Chem 287, 13620–13632.

Reichert H (2011). *Drosophila* neural stem cells: cell cycle control of self-renewal, differentiation, and termination in brain development. Results Probl Cell Differ 53, 529–546.

Rohatgi R, Milenkovic L, Scott MP (2007). Patched1 regulates hedgehog signaling at the primary cilium. Science 317, 372–376.

Ruat M, Roudaut H, Ferent J, Traiffort E (2012). Hedgehog trafficking, cilia and brain functions. Differentiation 83, S97–104.

Satir P, Pedersen LB, Christensen ST (2010). The primary cilium at a glance. J Cell Sci 123, 499–503.

Sauane M *et al*. (2010). Ceramide plays a prominent role in MDA-7/IL-24-induced cancer-specific apoptosis. J Cell Physiol 222, 546–555.

Smith L, Chen L, Reyland ME, DeVries TA, Talanian RV, Omura S, Smith JB (2000). Activation of atypical protein kinase C zeta by caspase processing and degradation by the ubiquitin-proteasome system. J Biol Chem 275, 40620–40627.

Smith L, Smith JB (2002). Lack of constitutive activity of the free kinase domain of protein kinase C zeta. Dependence on transphosphorylation of the activation loop. J Biol Chem 277, 45866–45873.

Smith L, Wang Z, Smith JB (2003). Caspase processing activates atypical protein kinase C zeta by relieving autoinhibition and destabilizes the protein. Biochem J 375, 663–671.
Spassky N, Han YG, Aguilar A, Strehl L, Besse L, Laclef C, Ros MR, Garcia-Verdugo JM, Alvarez-Buylla A (2008). Primary cilia are required for cerebellar development and Shh-dependent expansion of progenitor pool. Dev Biol 317, 246–259.
Stoffel W, Jenke B, Holz B, Binczek E, Gunter RH, Knifka J, Koebke J, Niehoff A (2007). Neutral sphingomyelinase (SMPD3) deficiency causes a novel form of chondrodysplasia and dwarfism that is rescued by Col2A1-driven smpd3 transgene expression. Am J Pathol 171, 153–161.
Sultan I, Senkal CE, Ponnusamy S, Bielawski J, Szulc Z, Bielawska A, Hannun YA, Ogretmen B (2006). Regulation of the sphingosine-recycling pathway for ceramide generation by oxidative stress, and its role in controlling c-Myc/Max function. Biochem J 393, 513–521.
Swistowski A, Peng J, Liu Q, Mali P, Rao MS, Cheng L, Zeng X (2010). Efficient generation of functional dopaminergic neurons from human induced pluripotent stem cells under defined conditions. Stem Cells 28, 1893–1904.
Toughiri R, Li X, Du Q, Bieberich CJ (2013). Phosphorylation of NuMA by Aurora-A kinase in PC-3 prostate cancer cells affects proliferation, survival, and interphase NuMA localization. J Cell Biochem 114, 823–830.
Valenzuela-Fernandez A, Cabrero JR, Serrador JM, Sanchez-Madrid F (2008). HDAC6: a key regulator of cytoskeleton, cell migration and cell-cell interactions. Trends Cell Biol 18, 291–297.
Wang G, Krishnamurthy K, Bieberich E (2009a). Regulation of primary cilia formation by ceramide. J Lipid Res 50, 2103–2110.
Wang G, Krishnamurthy K, Chiang YW, Dasgupta S, Bieberich E (2008). Regulation of neural progenitor cell motility by ceramide and potential implications for mouse brain development. J Neurochem 106, 718–733.
Wang G, Krishnamurthy K, Umapathy NS, Verin AD, Bieberich E (2009b). The carboxyl-terminal domain of atypical protein kinase Czeta binds to ceramide and regulates junction formation in epithelial cells. J Biol Chem 284, 14469–14475.
Wang G, Silva J, Krishnamurthy K, Tran E, Condie BG, Bieberich E (2005). Direct binding to ceramide activates protein kinase Czeta before the formation of a pro-apoptotic complex with PAR-4 in differentiating stem cells. J Biol Chem 280, 26415–26424.
Wu BX, Clarke CJ, Hannun YA (2010a). Mammalian neutral sphingomyelinases: regulation and roles in cell signaling responses. Neuromol Med 12, 320–330.
Wu BX, Rajagopalan V, Roddy PL, Clarke CJ, Hannun YA (2010b). Identification and characterization of murine mitochondria-associated neutral sphingomyelinase (MA-nSMase), the mammalian sphingomyelin phosphodiesterase 5. J Biol Chem 285, 17993–18002.
Xiong Y, Zhao K, Wu J, Xu Z, Jin S, Zhang YQ (2013). HDAC6 mutations rescue human tau-induced microtubule defects in *Drosophila*. Proc Natl Acad Sci USA 110, 4604–4609.
Yamada M, Hirotsune S, Wynshaw-Boris A (2010). The essential role of LIS1, NDEL1 and Aurora-A in polarity formation and microtubule organization during neurogenesis. Cell Adh Migr 4, 180–184.